Anal. Chem. **2009,** *81,* 6641–6648

Synthesis of Gelatin-Stabilized Gold Nanoparticles and Assembly of Carboxylic Single-Walled Carbon Nanotubes/Au Composites for Cytosensing and Drug Uptake

Jing-Jing Zhang, Miao-Miao Gu, Ting-Ting Zheng, and Jun-Jie Zhu*

Key Laboratory of Analytical Chemistry for Life Science (Ministry of Education of China), School of Chemistry and Chemical Engineering, Nanjing University, Nanjing 210093, P. R. China

Gelatin-stabilized gold nanoparticles (AuNPs-gelatin) with hydrophilic and biocompatible were prepared with a simple and "green" route by reducing in situ tetrachloroauric acid in gelatin. The nanoparticles showed the excellent colloidal stability. UV−vis spectra, transmission electron microscopy (TEM), and atomic force microscopy revealed the formation of well-dispersed AuNPs with different sizes. By combination of the biocompatibility of AuNPs and excellent conductivity of carboxylic single-walled carbon nanotubes (c-SWNTs), a novel nanocomposite was designed for the immobilization and cytosensing of HL-60 cells at electrodes. The immobilized cells showed sensitive voltammetric response, good activity, and increased electron-transfer resistance. It can be used as a highly sensitive impedance sensor for HL-60 cells ranging from 1×10^4 to 1×10^7 cell mL^{-1} with a limit of detection of 5×10^3 cell mL^{-1}. Moreover, the nanocomposite could effectively facilitate the interaction of adriamycin (ADR) with HL-60 cells and remarkably enhance the permeation and drug uptake of anticancer agents in the cancer cells, which could readily lead to the induction of the cell death of leukemia cells.

For the last 2 decades, there has been a considerable interest in the design of biosensors for the detection of cells and their activity monitoring. Some methods such as scanning electrochemical microscopy (SECM),[1] electrochemical impedance spectroscopy (EIS),[2] electric cell-substrate impedance sensing (ECIS),[3] and oxygen electrode[4] have been developed for monitoring cell viability and proliferation. Among these methods, electrochemical cell-based biosensors have attracted increasing attention due to their remarkable advantages such as low cost, convenient operation, rapid detection, and good sensitivity.[5−7] Anchoring cells on the electrode for producing electrochemical signals is a key step in the development of electrochemical biosensors. However, many limitations were observed during the immobilization of cells on electrode surface by conventional methods, such as instability, additional diffusional barrier, and decrease of cell viability.[8−10] Recent research has focused on the design of biomaterials for cell adhesion.[11−13]

With the development of nanoscience and nanotechnology, gold nanoparticles (AuNPs) have been extensively used as a matrix and cytochemical label for the respective cancer diagnostics and tumor target treatment.[14−16] To date, a variety of methods have been developed to generate monodisperse gold nanoparticles.[17−20] One of the most widely used methods is the reduction of tetrachloraurate ions by $NaBH_4$ or other reductive reagents. Recently, AuNPs synthesized with polymers as both the reducing and stabilizing agent were reported to improve their stability and biocompatibility and enhance the capability for the immobilization due to the superior properties of the formed nanocomposites.[21] Gelatin is the thermally and hydrolytically denatured product of collagen, which has been extensively applied as the immobilization matrix for the preparation of biosensors.[22,23] It has a triple-helical structure and

* To whom correspondence should be addressed.

(1) Kaya, T.; Torisawa, Y. S.; Oyamatsu, D. *Biosens. Bioelectron.* **2003**, *18*, 1379–1383.
(2) K'Owino, I. O.; Sadik, O. A. *Electroanalysis* **2005**, *17*, 2101–2113.
(3) Heiskanen, A. R.; Spegel, C. F.; Kostesha, N. *Langmur* **2008**, *24*, 9066–9073.
(4) Lahdesmaki, I.; Park, Y. K.; Carroll, A. D. *Analyst* **2007**, *132*, 811–817.
(5) Du, D.; Ju, H. X.; Zhang, X. J.; Chen, J.; Cai, J.; Chen, H. Y. *Biochemistry* **2005**, *44*, 11539–11545.
(6) Hua, H. L.; Jiang, H.; Wang, X. M.; Chen, B. A. *Electrochem. Commun.* **2008**, *10*, 1121–1124.
(7) Shen, Q.; You, S. K.; Park, S. G.; Jiang, H.; Guo, D. D.; Chen, B. A.; Wang, X. M. *Electroanalysis* **2008**, *20*, 2526–2530.
(8) Mulchandani, A.; Kaneva, I.; Chen, W. *Anal. Chem.* **1998**, *70*, 5042–5046.
(9) Muscat, A.; Beyersdorf, J.; Vorlop, K. D. *Biosens. Bioelectron.* **1995**, *10*, 11–14.
(10) Zheng, J.; Northrup, S. R.; Hornsby, P. J. *In Vitro Cell. Dev. Biol.: Anim.* **1998**, *34*, 679–684.
(11) Ionescu, R. E.; Abu-Rabeah, K.; Cosnier, S. *Electroanalysis* **2006**, *18*, 1041–1046.
(12) Zhang, Z.; Chen, S. F.; Jiang, S. Y. *Biomacromolecules* **2006**, *7*, 3311–3315.
(13) Gu, H. Y.; Chen, Z.; Sa, R. X. *Biomaterials* **2004**, *25*, 3445–3451.
(14) Giljohann, D. A.; Seferos, D. S.; Patel, P. C.; Millstone, J. E.; Rosi, N. L.; Mirkin, C. A. *Nano Lett.* **2007**, *7*, 3818–3821.
(15) Souza, G. R.; Christianson, D. R.; Staquicini, F. I.; Ozawa, M. G.; Snyder, E. Y.; Sidman, R. L.; Miller, J. H.; Arap, W.; Pasqualini, R. *Proc. Natl. Acad. Sci. U.S.A.* **2006**, *103*, 1215–1220.
(16) Murphy, C. J. *Nano Lett.* **2007**, *7*, 116–119.
(17) Guo, S. J.; Wang, E. K. *Inorg. Chem.* **2007**, *46*, 6740–6743.
(18) Zheng, N.; Fan, J.; Stucky, G. D. *J. Am. Chem. Soc.* **2006**, *128*, 6550–6551.
(19) Lu, X. M.; Tnan, H. Y.; Korgel, B. A. *Chem.—Eur. J.* **2008**, *14*, 1584–1591.
(20) Li, Z. G.; Friedrich, A.; Taubert, A. *J. Mater. Chem.* **2008**, *18*, 1008–1014.
(21) Sardar, R.; Park, J. W.; Shumaker-Parry, J. S. *Langmuir* **2007**, *23*, 11883–11889.
(22) Li, N.; Xu, J. Z.; Yao, H.; Zhu, J. J.; Chen, H. Y. *J. Phys. Chem. B* **2006**, *110*, 11561–11565.

10.1021/ac900628y CCC: $40.75
Published on Web 07/14/2009

offers distinctive advantages such as good biocompatibility, nontoxicity, remarkable affinity to proteins, and excellent gel-forming ability. To the best of our knowledge, there is no report on the use of gelatin as a reducing and stabilizing agent to prepare AuNPs-embedded gelatin nanocomposites (AuNPs-gelatin). In this study, AuNPs were prepared in situ in gelatin solution without the use of an additional stabilizing agent. The major advantage for gelatin as a stabilizing agent is that it can be used to tailor the nanocomposite properties and also to provide long-term stability of the nanoparticles by preventing particle agglomeration. This method did not introduce any environmental toxicity or biological hazards and thus was simple and "green".

Single-wall carbon nanotubes (SWNTs) with their unique one-dimensional hollow nanostructure and unusual properties are emerging as an important new class of multifunctional building blocks in electrochemistry, biomedical engineering, and medical chemistry.[24−27] Particularly in electrochemistry, the high-aspect ratios of the tubes may present a steric effect for more efficient redox reactions of biomolecules. Hence, the excellent conductivity of SWNTs is beneficial to the design of the novel biomaterials for the determination of dopamine,[28] explosive nitroaromatic compounds,[29] hydrogen peroxide,[30] and DNA.[31] Moreover, SWNTs have recently been developed as contrast agents in cancer targeting, imaging and for the delivery of therapeutically active drugs to target cells.[32−36] In these drug delivery systems, SWNTs could provide very high surface area per unit weight for high drug loading and transport across cell membranes with little cytotoxicity. Compared to these delivery systems, we provided the first demonstration that carboxylic single-walled carbon nanotubes (c-SWNTs) and gelatin-stabilized gold nanoparticles may have a cooperative effect in facilitating the uptake of anticancer drug ADR into the targeted tumor cells.

In this work, by combination of the gelatin-stabilized gold nanoparticles and c-SWNTs, a novel nanocomposite with c-SWNTs-AuNPs-gelatin was assembled to construct a nontoxic biomimetric interface for the immobilization of HL-60 cells on the electrode surface. The immobilized cells exhibited an irreversible voltammetric response and good activity of living cells. By the aid of the use of impedance spectroscopy, the modified electrode can offer an extremely sensitive biosensing for the determination of cell concentration ranging from 1×10^4 to 1×10^7 cell mL^{-1} with a limit of detection of 5×10^3 cell mL^{-1} at 3σ. Furthermore, the results of cytotoxicity (MTT) assays showed that the c-SWNTs and AuNPs-gelatin could effectively facilitate the interaction of adriamycin (ADR) with HL-60 cells and contribute to their beneficial effects on intracellular drug uptake of HL-60 cells, suggesting a potential application of the nanocomposites in cytosensing and cancer diagnostic.

EXPERIMENTAL SECTION

Reagents. SWNTs with purity level above 90%, length 0.5−2 μm, and diameter 1−2 nm were obtained from Chengdu Organic Chemicals Co. Ltd. and were further functionalized with a carboxyl group to increase their solubility in aqueous solution by sonicating in a mixture of HNO_3 and H_2SO_4 (1:3, v/v) for 6 h and washed with water and then dried at 60 °C. The shortened length of c-SWNTs was in the range of 50−150 nm (see Supporting Information, Figure S1). $HAuCl_4 \cdot 4H_2O$ (Au% > 48%) and the gelatin were from Shanghai Chemical Reagent Co. (Shanghai, China). Adriamycin was purchased from Sigma-Aldrich (St. Louis, MO). Phosphate buffer saline (PBS, pH 7.0) contained 137 mM NaCl, 2.7 mM KCl, 87 mM Na_2HPO_4, and 14 mM KH_2PO_4. The pH value of PBS was adjusted by changing the ratio of Na_2HPO_4 to KH_2PO_4. The ionic strength of electrolyte solutions was adjusted by adding sodium chloride in pH 7.0 PBS. All other chemicals were of analytical grade, and all aqueous solutions were prepared with doubly distilled water.

Preparation of Gold Nanoparticles-Embedded Gelatin Nanocomposite Sol. All glassware used in the experimental procedures was cleaned in a bath of freshly prepared HNO_3/HCl (3:1, v/v), rinsed thoroughly in doubly distilled water, and dried prior to use. Gold nanoparticles (AuNPs) with various diameters were prepared using gelatin as reducing/stabilizing reagent. The aqueous gelatin solution with 20 mL (3%, wt %) was heated to 80 °C. When stirred vigorously, 2.0 mL of the $HAuCl_4$ solution (1%, wt %) was added rapidly. The mixed solution was shaken vigorously for 30 s and left undisturbed for 2 h at 80 °C, at which a red AuNPs-gelatin solution was obtained.

Electrode Modification with c-SWNTs-AuNPs-Gelatin Composite Films. The glass carbon electrode (GCE) was first polished with 1.0, 0.3, and 0.05 μm α-alumina powder and sonicated in acetone and water successively. Finally, the GCE was thoroughly rinsed with water and dried at room temperature. For the preparation of c-SWNTs-AuNPs-gelatin/GCE, 5 μL of 100 μg mL^{-1} c-SWNTs was first mixed with 5 μL of AuNPs-gelatin solution and sonicated at room temperature for 2 h. Then, 5 μL of the solution with the nanocomposites was dropped on the pretreated GCE and dried in a silica gel desiccator. The modified electrodes were stored in air prior to use.

Cell Culture and Immobilization. The cell line HL-60 was provided by HL60 cells which were cultured in a flask in RPMI 1640 medium (Gibco, Grand Island, NY) supplemented with 10% fetal calf serum (FCS, Sigma), penicillin (100 μg mL^{-1}), and streptomycin (100 μg mL^{-1}) in an incubator (5% CO_2, 37 °C). After cultured for 72 h, the cells were collected and separated from the medium by centrifugation at 1000 rpm for 10 min and

(23) Yao, H.; Li, N.; Xu, J. Z.; Zhu, J. J. *Talanta* **2007**, *71*, 550–554.
(24) Luo, H. X.; Shi, Z. J.; Li, N. Q.; Gu, Z. N.; Zhuang, Q. K. *Anal. Chem.* **2001**, *73*, 915–920.
(25) Gan, Z. H.; Zhao, Q.; Gu, Z. N.; Zhuang, Q. K. *Anal. Chim. Acta* **2004**, *511*, 239–247.
(26) Zhu, L. D.; Yang, R. L.; Zhai, J. G.; Tian, C. Y. *Biosens. Bioelectron.* **2007**, *23*, 528–535.
(27) Qiu, J. D.; Xie, H. Y.; Liang, R. P. *Microchim. Acta* **2008**, *162*, 57–64.
(28) Ali, S. R.; Ma, Y. F.; Parajuli, R. R.; Balogun, Y.; Lai, W. Y. C.; He, H. X. *Anal. Chem.* **2007**, *79*, 2583–2587.
(29) Hrapovic, S.; Majid, E.; Liu, Y.; Male, K.; Luong, J. H. T. *Anal. Chem.* **2006**, *78*, 5504–5512.
(30) Sun, N. J.; Guan, L. H.; Shi, Z. J.; Li, N. Q.; Gu, Z. N.; Zhu, Z. W.; Li, M. X.; Shao, Y. H. *Anal. Chem.* **2006**, *78*, 6050–6057.
(31) Wang, J. X.; Li, M. X.; Shi, Z. J.; Li, N. Q.; Gu, Z. N. *Electroanalysis* **2004**, *16*, 140–144.
(32) Jin, H.; Heller, D. A.; Strano, M. S. *Nano Lett.* **2008**, *8*, 1577–1585.
(33) Welsher, K.; Liu, Z.; Daranciang, D.; Dai, H. J. *Nano Lett.* **2008**, *8*, 586–590.
(34) MacDonald, R. A.; Laurenzi, B. F.; Viswanathan, G.; Ajayan, P. M.; Stegemann, J. P. *J. Biomed. Mater. Res., A* **2005**, *74A*, 489–496.
(35) Bhirde, A. A.; Patel, V.; Gavard, J.; Zhang, G. F.; Sousa, A. A.; Masedunskas, A.; Leapman, R. D.; Weigert, R.; Gutkind, J. S.; Rusling, J. F. *ACS Nano* **2009**, *3*, 307–316.
(36) Chen, J. Y.; Chen, S. Y.; Zhao, X. R.; Kuznetsova, L. V.; Wong, S. S.; Ojima, I. *J. Am. Chem. Soc.* **2008**, *130*, 16778–16785.

then washed twice with a sterile pH 7.0 PBS. The sediment was suspended in the PBS to obtain a homogeneous cell suspension with the final concentration of 5.0×10^6 cells mL^{-1}, which was determined by using a Petroff-Hausser cell counter. The cell suspensions with various contents were prepared from this stock. Then 5 μL of the cell suspension was dropped on the c-SWNTs-AuNPs-gelatin-modified GCE and was incubated at 37 °C for 2 h to achieve cell immobilization.

Inverted Fluorescence Microscopy Studies. Initially, the leukemia HL-60 cells (1×10^6 cells per well) were inoculated into 24-well flat-bottomed plates and grown for 24 h. Then, ADR, c-SWNTs, and AuNPs-gelatin dispersion were injected into the cell culture for incubation. The concentration of ADR was controlled at 20 μg mL^{-1} and that of c-SWNTs and AuNPs-gelatin was 9 μg mL^{-1}. After cultured for 6 h, the cells were collected and separated from the medium by centrifugation at 1000 rpm for 10 min. The supernatant solution was used for electrochemical detection of ADR, and the sediment was suspended in the PBS and dropped on a strictly cleaned glass plate for inverted fluorescence microscopy (DMLP, Leica) imaging. The excitation wavelength of fluorescence was adjusted at 550 nm. In control experiments, only ADR was injected.

MTT Assays. The inhibition of cell growth was measured by a MTT assay. Briefly, HL-60 cells were plated at a density of 1×10^4 cells per well in 100 μL of RPMI 1640 medium in 96-well plates and grown for 24 h. The cells were then exposed to 10 μL of ADR (10 μg mL^{-1}) and a series of concentrations of c-SWNTs and AuNPs-gelatin for 24 h, and the viability of the cells was measured using the methylthiazoletetrazolium method. Each experiment was repeated at least four times. Controls were cultivated under the same conditions without the addition of the nanocomposites. Then, 5 μL of MTT (5 mg mL^{-1}) was added into the wells and further incubated for an additional 4 h. Subsequently, it was centrifuged at 1000 rpm for 10 min and the supernatant was discarded, followed by the addition of 100 μL of DMSO into each well and incubation in the shaker incubator with gentle shakes. Then the optical density (OD) was read at a wavelength of 570 nm. Relative inhibition of cell growth was expressed as follows: $\% = (1 - [OD]_{test}/[OD]_{control}) \times 100$.

Apparatus and Characterizations. UV−vis spectra were recorded on a UV-3600 spectrophotometer (Shimadzu, Kyoto, Japan). Transmission electron micrographs (TEM) were measured on a JEOLJEM 200CX transmission electron microscope, using an accelerating voltage of 200 kV. The static water contact angles were measured at 25 °C by a contact angle meter (Rame-Hart-100) employing drops of pure deionized water. The readings were stabilized and taken within 120 s after the addition. Atomic force microscopy (AFM) images were obtained on a SPI3800 controller operated in tapping mode with an acquisition frequency of 1.5 Hz and line density of 512.2×2 μm scans. Fourier transform infrared (FT-IR) spectra were recorded on a Vector 22 FT-IR spectrometer (Bruker). Samples were thoroughly ground with exhaustively dried KBr.

Electrochemical Measurements. Electrochemical measurements were performed on a CHI 660a workstation (Shanghai Chenhua, Shanghai, China) in pH 7.0 PBS with a conventional three-electrode system comprised of a platinum wire as the auxiliary, a saturated calomel electrode as the reference, and the modified GCE as the working electrode. Electrochemical impedance spectroscopy (EIS) was performed with an Autolab electrochemical analyzer (Eco Chemie, The Netherlands) in a 10 mM $K_3Fe(CN)_6/K_4Fe(CN)_6$ (1:1) mixture with 1.0 M KCl as the supporting electrolyte, using an alternating current voltage of 5.0 mV, within the frequency range of 0.01 Hz−100 kHz. All of the experiments were performed at 37 ± 0.5 °C.

Scheme 1. Gelatin-Induced Synthesis and Stabilization of Gold Nanoparticles in Water

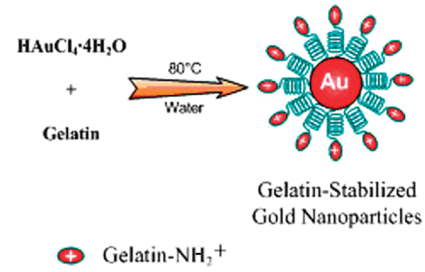

RESULTS AND DISCUSSION

Preparation and Characterization of AuNPs-Gelatin and c-SWNTs-AuNPs-Gelatin Nanocomposites. In the case of gold nanoparticles, the synthesis was performed. In the reaction, the gelatin as both a reducing and a stabilizing agent is shown in Scheme 1. When $HAuCl_4$ solution was mixed with gelatin solution at a temperature of 80 °C, the solution remained colorless in the initial 20 min, then it turned light purple slowly, and at 120 min the final solution became red.

After reaction at 80 °C for 120 min, the obtained gold nanoparticles exhibited a UV−vis absorption peak centered at 530 nm (curve a, Figure 1A), a typical surface plasmon resonance band for AuNPs, while no absorption was observed for the gelatin solution (curve b, Figure 1A). The TEM image showed that the as-prepared AuNPs was uniform spheres with a diameter of 10−20 nm (inset of Figure 1A). UV−vis absorption spectroscopy was also used to monitor the preparation of AuNPs at different stages. As shown in Figure 1B, the intensity of the surface plasmon absorption increased with the increase of reaction time, which indicated the continued reduction of the metal ions. The light purple solution collected at 40 min (curve b) showed a broad peak maximum, λ_{max}, at 594 nm, which is characteristic for AuNPs in this size regime and dielectric environment.[37] When the reaction time reached 60 min (curve c), the λ_{max} value was blue-shifted by 17 to 577 nm. At the end of the reduction (curve h), there was only a single sharp peak with the λ_{max} value of 530 nm, which is a 7 nm blue-shifted from 537 nm for the purple-red colored solution (curve f). This blue-shift is likely due to the dissociation of larger particles into smaller particles. At the initial stage of the reaction, the AuNPs aggregated together with a broad size distribution, which led to a broad UV−vis absorption peak at about 600 nm. After this stage, the aggregated particles could dissociate due to heating to form smaller particles stabilized by the amine pendant groups on the gelatin backbone, which leads to the formation of gelatin-stabilized stable gold nanoparticles. The mechanism of the gold

(37) Ding, Y.; Zhang, X.; Liu, X.; Guo, R. *Colloids Surf., A* **2006**, *290*, 82–88.

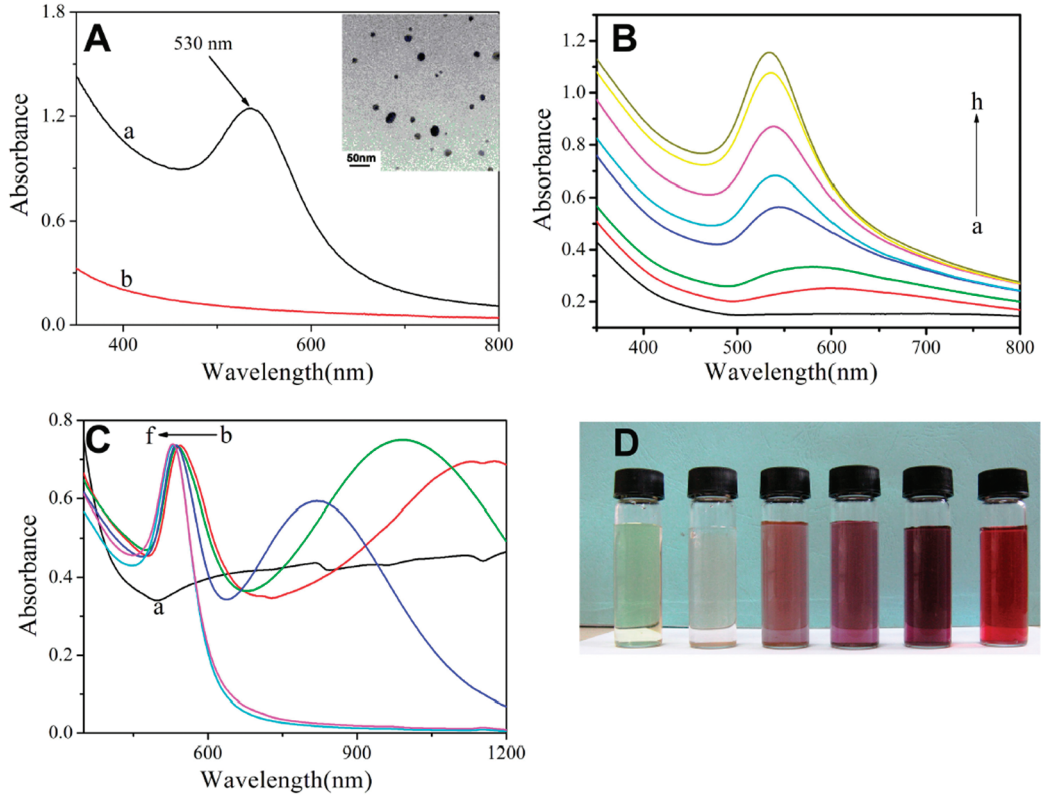

Figure 1. (A) UV−visible absorption spectra of AuNPs-gelatin (a) and pure gelatin solution (b). Inset: TEM image of the obtained AuNPs. (B) Time evolution of the surface plasmon absorption spectra of the AuNPs-gelatin. The time intervals are (a) 20, (b) 40, (c) 60, (d) 80, (e) 100, (f) 110, and (g) 120 min. (C) UV−visible absorption spectra of AuNPs-gelatin synthesized with varying amounts of gelatin solution: (a) 0.25%, (b) 0.5%, (c) 0.75%, (d) 1%, (e) 2%, and (f) 4%. (D) Optical images of the gelatin solution and AuNPs-gelatin synthesized with 0.25%, 0.5%, 0.75%, 1%, and 2% gelatin solutions (from left to right).

reduction process can be explained by the metal ion-induced oxidation of amine to nitrite, which has been described previously.[38]

The formation of AuNPs in the presence of different gelatin concentrations were further investigated (0−4%, wt %). The AuNPs was monitored by UV−vis absorption spectroscopy. According to the UV−vis spectrum shown in Figure 1C, the maximum absorption wavelength increased with the decrease of reductant gelatin concentrations. The dependence of the λ_{max} on the reductant gelatin is similar to the report in the luminal reduction method.[39] Figure 1D showed the distinct color change corresponding to the UV−vis results. Because gelatin gel is a semitransparent white gel, with the increase of gelatin, the formed AuNPs-gelatin showed a distinct color change from light purple, purple, dark purple, red wine, and red, respectively (from left to right). Those AuNPs with gelatin were stable in water more than 6 months at room temperature without observable precipitation. In addition, since only nontoxic materials and solvent were used in the synthesis, it is thought viable to readily integrate these particles into a variety of systems, especially those that are relevant to biological and biomedical applications.

The morphology of the AuNPs was observed by AFM. As observed in Figure 2, the pure gelatin film displayed a uniformly distributed and intact surface with a height less than 6 nm (Figure 2A), while the AuNPs-gelatin film showed a densely packed structure with a height of 33 nm (Figure 2B). The AuNPs in the film are connected to each other, resulting in a nanosized concave−convex surface, which is somewhat similar to micropattern surfaces.[40] Thus, the AuNPs-gelatin film could provide a biocompatible and rough surface for cell immobilization. However, the coexisted gelatin film may somewhat block the electron transfer. Therefore, novel nanocomposites were further fabricated to improve the conductivity. The first approach was the oxidation of the SWNTs surface to create functional carboxylic groups and increase the solubility. The TEM image illustrated that the length of obtained c-SWNTs was in the range of 50−150 nm (Figure S1 in the Supporting Information). The presence of carboxylic groups on the surface of c-SWNTs was confirmed by FT-IR spectra. As shown in Figure S2 in the Supporting Information, the appearance of the peaks (1720, 1580 cm^{-1}) corresponded to the carboxylic acid group and the carboxylate group, respectively. The second procedure involved the incorporation of c-SWNTs with AuNPs-gelatin by sonication protocol. Details of the fabrication of c-SWNTs-AuNPS-gelatin nanocomposites were given in the Experimental Section. Figure 2C showed the TEM image of the as-prepared c-SWNTs-AuNPs-gelatin nanocomposites. Because of the charge interactions as well as other possible cooperation binding forces, it was possible to incorporate the c-SWNTs into the AuNPs-gelatin film. However, the c-SWNTs agglomerated to

(38) Capdevielle, P.; Lavigne, A.; Sparfel, D.; Lafont-Baranne, J.; Cuong, N. K.; Maumy, M. *Tetrahedron Lett.* **1990**, *31*, 3305–3308.
(39) Cui, H.; Wang, W.; Duan, C. F.; Dong, Y. P.; Guo, J. Z. *Chem.—Eur. J.* **2007**, *13*, 6975–6984.
(40) Amirpour, M. L.; Ghosh, P.; Lackowski, W. M.; Crooks, R. M.; Pishko, M. V. *Anal. Chem.* **2001**, *73*, 1560–1566.

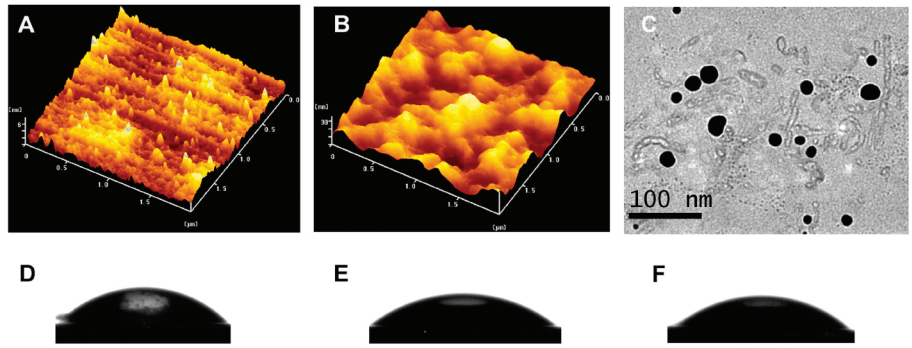

Figure 2. AFM images of the pure gelatin film (A) and AuNPs-gelatin film (B). (C) TEM image of c-SWNTs-AuNPs-gelatin nanocomposites. Contact angle of GCE modified with pure gelatin film (D), AuNPs-gelatin film (E), and c-SWNTs-AuNPs-gelatin film (F).

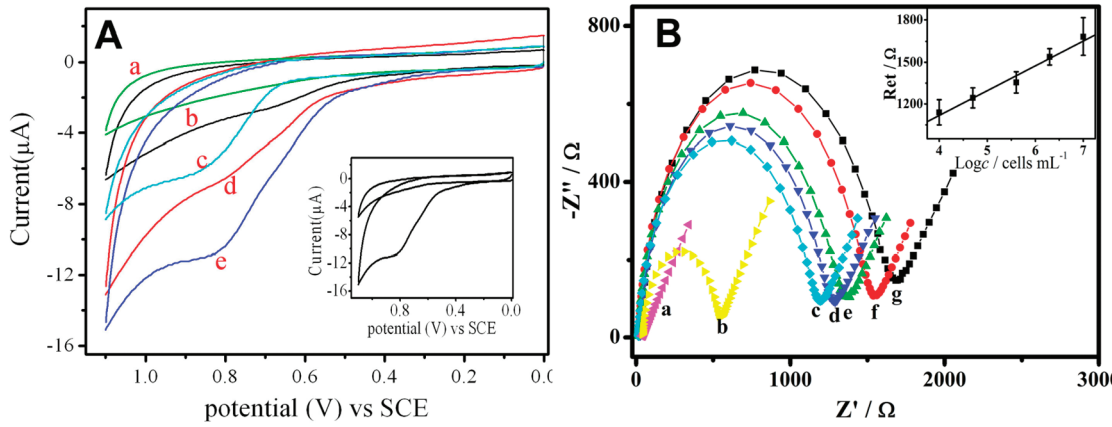

Figure 3. (A) Cyclic voltammograms of (a) bare GCE, (b) c-SWNT-AuNPs-gelatin /GCE in pH 7.0 PBS, (c) c-SWNT-AuNPs-gelatin/GCE in pH 7.0 PBS containing 1.0 μg/mL guanine, (d) HL-60 cells/GCE, (e) HL-60 cells/c-SWNT-AuNPs-gelatin/GCE in pH 7.0 PBS. Inset: two continuous sweeps of curve e. Scan rate: 100 mV s^{-1}. (B) Nyquist diagrams of electrochemical impedance spectra recorded from 0.1 to 10^6 Hz for $[Fe(CN)_6]^{3-}$/$[Fe(CN)_6]^{4-}$ (10 mM, 1:1) in 1.0 M KCl at a bare GCE (a), c-SWNT-AuNPs-gelatin/GCE (b), and HL-60/c-SWNT-AuNPs-gelatin/GCE with the cell concentrations of 1.0×10^4, 5.0×10^4, 4.0×10^5, 2.0×10^6, and 1.0×10^7 cells mL^{-1} (from curves c to g).

some extent and some free gold nanoparticles were observed in the background of the TEM micrograph. The nanocomposites combined the biocompatibility of AuNPs and excellent conductivity of c-SWNTs, thus it not only offered a biocompatible surface but also acted as an analogue of extracellular matrix to induce cell adhesion effectively.

The hydrophilicity of the films was characterized by measuring the contact angle of pure gelatin, AuNPs-gelatin, and c-SWNTs-AuNPs-gelatin. As shown in Figure 2, the contact angles of the three films were 44.9°, 39.5°, and 36.8°, respectively. The c-SWNTs-AuNPs-Gelatin nanocomposites showed the lowest contact angle, indicating better hydrophilicity, which may be attributed to the carboxylic and carboxylate groups of c-SWNTs. Thus, the c-SWNTs-AuNPs-gelatin nanocomposites could provide a biocompatible surface, which was in favor of promoting cell adhesion and growth.

Cyclic Voltammetric Behavior of HL-60 Cells at the Nanocomposites-Modified Electrode. Electron generation and charge transfer exist in all living cells due to the redox reactions and the changes of ionic composition and concentration in life processes.[41] As shown in Figure 3A, no detectable cyclic voltammetric response was observed for the bare GCE and the c-SWNTs-AuNPs-gelatin/GCE, respectively. The latter displayed a larger background current due to the larger accessible surface area of the modified electrode. After the immobilization of HL-60 cells at the c-SWNTs-AuNPs-gelatin/GCE, a well-defined oxidation peak appeared at + 0.84 V at 100 mV s^{-1}. No corresponding reduction wave was observed in the reverse scan, and the oxidation peak decreased greatly or disappeared in the second scan. Furthermore, the voltammogram of c-SWNTs-AuNPs-gelatin/GCE in pH 7.0 PBS containing 1.0 μg mL^{-1} guanine also showed an irreversible peak at the potential close to that observed at HL-60/c-SWNTs-AuNPs-gelatin/GCE, indicating that the irreversible oxidation peak was possibly attributed to the conversion of guanine in cell cytoplasm to 8-oxo-guanine.[42] However, after the same procedures were performed at the GCE without the presence of c-SWNTs-AuNPs-gelatin nanocomposites, no amperometric signal was observed, indicating the need of biocompatible and hydrophilic nanocomposite matrix for cell adhesion. The results revealed that the c-SWNTs on the nanocomposites-modified electrode could act as an electron conductor for promoting electron-transfer reactions between electroactive centers of cells and the electrode, while the AuNPs-gelatin could greatly improve the biocompatibility and hydrophilicity of the electrode for cell adhesion.

Optimization of the Experimental Conditions. The electrochemical performance of the cell sensor mainly depended on

(41) Nonner, W.; Eisenberg, B. *J. Mol. Liq.* **2000**, *87*, 149–162.

(42) Feng, J.; Ci, Y. X.; Lou, J. L.; Zhang, X. Q. *Bioelectrochem. Bioenerg.* **1999**, *48*, 217–222.

Table 1. Comparison of the Developed Cell Sensor with Other CNTs-AuNPs-Based Sensors

sensor fabrication[a]	analyte	linear range	detection limit	ref
Fc-pepstatin/SWCNT/AuNP/Au	HIV-1 PR	0.5−80 pM	0.8 pM	46
goat anti-HIgG/GNPs/CNTs/GCE	HIgG	0.125−80 ng mL^{-1}	40 pg mL^{-1}	47
ssDNA/Au_{nano}-CNT/PAN_{nano}/CPE	DNA	1.0 pM−1.0 μM	0.56 pM	48
AFP/GNP/CNT/Ch/GC	AFP	1−55 ng mL^{-1}	0.6 ng mL^{-1}	49
c-SWNTs-AuNPs-gelatin/GCE	HL-60	$(1 \times 10^4)-(1 \times 10^7)$ cell mL^{-1}	5×10^3 cell mL^{-1}	this work

[a] Fc, ferrocene; Au, gold electrode; HIV-1 PR, human immunodeficiency virus type-1 protease; HIgG, human IgG; PAN_{nano}, polyaniline nanofibers; CPE, carbon paste electrode; AFP, α-fetoprotein; Ch, chitosan.

the component of the nanocomposites. Figure S3 in the Supporting Information shows the dependence of the reduction peak current of ferricyanide under different experimental variables, containing c-SWNTs concentration in a c-SWNT-AuNPs-gelatin nanocomposite film and AuNPs synthesized by different gelatin concentrations. As shown in Figure S3A in the Supporting Information, with the formation of a AuNPs-gelatin film at GCE, the reduction peak current decreased greatly, while the incorporation of c-SWNTs in the AuNPs-gelatin film could increase the reduction peak, indicating that c-SWNTs could improve the conductivity of the c-SWNT-AuNPs-gelatin nanocomposite film. With the increasing concentration of c-SWNTs, the reduction peak current increased at first and leveled off between 100 and 150 $\mu g\ mL^{-1}$ (Figure S3B in the Supporting Information). Considering the fact that excessive c-SWNTs will affect the stability of the nanocomposite film and was unsuitable for the adhesion of cells, a concentration of 100 $\mu g\ mL^{-1}$ was chosen.

Effects of AuNPs synthesized by different gelatin concentrations on reduction peak current were also investigated, as shown in Figure S3C in the Supporting Information. With enhancement of the concentration of gelatin, the reduction peak current increased and approached a constant value. When its amount was too much it will block the electron transfer as it could form a thick film on the electrode surface. However, when the c-SWNTs were incorporated with the AuNPs synthesized by 2 wt % gelatin, the nanocomposites film formed was unstable. Considering the stability and conductivity of the nanocomposites film, the optimal concentration of gelatin was selected as 3 wt % in this work. Thus, under the optimized conditions, the obtained nanocomposites film was stable enough for the adhesion and detection of cells.

Impedance Sensor for HL-60 Cells. Impedance technique is an alternative to develop biosensors for the detection of cells.[43−45] The electron-transfer impedance (Ret) of the redox probe at the electrodes relied on the modification and the presence of living cells. As shown in Figure 3B, the Ret value of bare GCE was 16 Ω (curve a). Upon the assembly of a nanocomposites layer on the electrode surface, the Ret increased to 363 Ω (curve b) because the coexisted gelatin films acted as a barrier to the interfacial electron transfer. After the immobilization of cells, a barrier would hamper the redox probe close to the electrode surface and further increased the value of Ret. The increasing impedance of Ret was related to the surface coverage of the cells on the electrode. Because of the excellent biocompatibility and conductivity of the nanocomposites, the modified electrode could offer a promising interface for the immobilization of HL-60 cells, which is suitable for sensitive detection of cells. Under optimized conditions, a linear relationship between the Ret and logarithmic value of HL-60 cells concentration was found in the range of 1×10^4 to 1×10^7 cell mL^{-1}. The linear regression equation was $R_{et}(\Omega) = 404.3 + 178.2 \log C_{cells}$ (cells mL^{-1}) with a correlation coefficient 0.988 ($n = 5$). The detection limit was estimated to be 5×10^3 cell mL^{-1}, at which the increase of the Ret value was 3 times the standard deviation of Ret detected at the c-SWNTs-AuNPs-gelatin/GCE.

The relative standard deviation (RSD), estimated from the slopes of the calibration plots of six freshly prepared c-SWNTs-AuNPs-gelatin modified electrodes, was 3.4%, showing good fabrication reproducibility. At the cell concentration of 3×10^4 cell mL^{-1}, the RSD of the prepared sensors was 5.4%. The stability of the c-SWNTs-AuNPs-gelatin/GCE was investigated when stored in a desiccator. After 1 month, the impedance response was still retained at 90% value of the initial response, showing good storage stability.

Additionally, the analytical performance of the developed cell sensor has been compared with those of other electrochemical sensors based on CNTs and AuNPs reported in the literatures. The fabrication characteristics are summarized in Table 1.[46−49] As can be seen, the proposed sensor exhibit a wide linear range and low detection limit for cancer cells. The reason might be the fact that the c-SWNTs-AuNPs-gelatin nanocomposites have excellent biocompatibility and conductivity and could greatly improve the sensitivity of the cell sensor. Thus, the presented strategy could afford a simple and applicable way for cancer cell quantification with acceptable sensitivity, stability, and reproducibility.

Viability of Cells Exposed to c-SWNTs-AuNPs-Gelatin Nanocomposites. The toxicity or biocompatibility of c-SWNTs-AuNPs-gelatin nanocomposites was studied by incubating them with HL-60 cells at 37 °C for 24 h. The in vitro cytotoxicity of the various concentrations for the nanocomposites was evaluated using a colorimetric cell-viability (MTT) assay shown in Figure 4A. In the MTT assay, the absorbance of formazan (produced by the cleavage of MTT by dehydrogenases in living cells) at 570 nm is directly proportional to the number of live cells. It can be clearly seen that cells incubated by using the nanocomposites with various concentration had some slightly low value but no signifi-

(43) Guo, M. L.; Chen, J. H.; Yun, X. B.; Chen, K.; Nie, L. H.; Yao, S. Z. *Biochim. Biophys. Acta* **2006**, *1760*, 432–439.
(44) Ding, L.; Hao, C.; Xue, Y. D.; Ju, H. X. *Biomacromolecules* **2007**, *8*, 1341–1346.
(45) Hao, C.; Ding, L.; Zhang, X. J.; Ju, H. X. *Anal. Chem.* **2007**, *79*, 4442–4447.
(46) Mahmoud, K. A.; Hrapovic, S.; Luong, J. H. T. *ACS Nano* **2008**, *2*, 1051–1057.
(47) Cui, R. J.; Huang, H. P.; Yin, Z. Z.; Gao, D.; Zhu, J. J. *Biosens. Bioelectron.* **2008**, *23*, 1666–1673.
(48) Zhou, N.; Yang, T.; Jiang, C.; Du, M.; Jiao, K. *Talanta* **2009**, *77*, 1021–1026.
(49) Lin, J. H.; He, C. Y.; Zhang, L. J.; Zhang, S. S. *Anal. Biochem.* **2009**, *384*, 130–135.

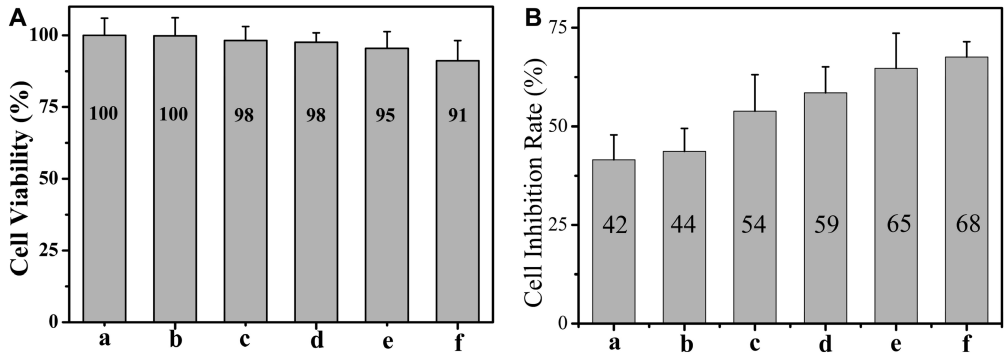

Figure 4. (A) Cytotoxicity studies of HL-60 cells treated with different concentrations of c-SWNTs and AuNPs-gelatin: (a) 0. (b) 0.5, (c) 1, (d) 2, (e) 5, and (f) 10 μg mL^{-1}. (B) MTT assays on the inhibition rate of leukemia HL-60 cells after treatment with ADR (1 μg mL^{-1}) and different concentrations of c-SWNTs and AuNPs-gelatin: (a) 0, (b) 0.5, (c) 1, (d) 2, (e) 5, and (f) 10 μg mL^{-1}.

cant difference in viability compared to controls at concentrations from 0.5 to 10.0 μg mL^{-1}. Thus the nanocomposites are nontoxic and may be used for in vivo animal studies and clinical research although detailed toxicity studies should be used to verify this point.

Cytotoxic assays were further used to determine the possibility of the utilization of the nanocomposites to increase the local drug delivery into the cancer cells. As shown in Figure 4B, the inhibition rates for the cell system cultured with 1 μg mL^{-1} ADR alone was 42%. However, the cell inhibition with the same ADR concentration in the presence of nanocomposites remarkably increased. With the increase of the concentration from 0.5 to 10.0 μg mL^{-1}, the cell inhibition rates increased from 44% to 68%, indicating the synergetic effect of the novel c-SWNTs-AuNPs-gelatin on the permeation and accumulation of ADR in the leukemia cells.

Inverted fluorescence microscopy was further utilized to image the intracellular fluorescence, which resulted from the drug uptake of ADR in leukemia HL-60 cells in the absence and presence of c-SWNTs and AuNPs-gelatin nanocomposites. As shown in Figure 5, when the leukemia HL-60 cells were treated by ADR alone, most of the cells showed weak red fluorescence, indicating that ADR molecules can approach and enter into the cell so that the cell image could be observed through the relative fluorescence of absorbed ADR. The average fluorescence intensity was calculated to be 50.9 by sampling the fluorescence of each image and transforming the color value of each pixel to a gray value with the software. However, when c-SWNTs and AuNPs-gelatin nanocomposites were introduced into the leukemia cells, the number of cells with high red fluorescence increased and the average intracellular fluorescence intensity produced 40% enhancement compared to the case of the cells treated with ADR alone. Since c-SWNTs and AuNPs-gelatin have no fluorescent properties under the related experimental conditions, the intracellular fluorescence was only generated by the anticancer drug ADR. Thus, it is evident that the c-SWNTs and AuNPs-gelatin could remarkably facilitate the drug uptake and accumulation of ADR into leukemia cancer cells and could thus act as an efficient agent to enhance drug delivery.

Moreover, the electrochemical studies provided the additional fresh evidence for the synergistic effect of the c-SWNTs and AuNPs-gelatin on the effective uptake of ADR into leukemia HL-60 cells. As we know, the ADR is an electroactive substance and

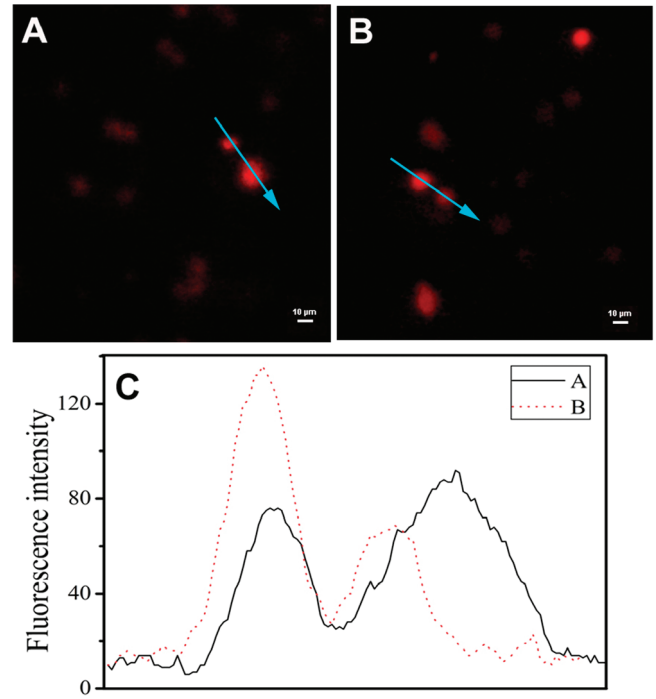

Figure 5. Inverted fluorescence micrographs of leukemia HL-60 cells after incubation with ADR in the absence (A) and presence of c-SWNTs and AuNPs-gelatin (B). (C) The comparison of the corresponding intracellular fluorescence intensity of leukemia HL-60 cells. The arrows illustrate the direction of sampling. The concentration of ADR was controlled at 20 μg mL^{-1} and that of c-SWNTs and AuNPs-gelatin was 9 μg mL^{-1}. Scale bar = 10 μm.

the redox centers are quinone and hydroquinone groups.[50] Correspondingly, in the cyclic voltammogram of ADR alone (curve a, Figure 6A), two pairs of redox peaks with medium potentials −0.65 and +0.38 V were observed, which correspond to the reduction of quinone (1) and the oxidation of hydroquinone (2) centers. These electrode reactions are shown in Figure 6B. After incubation of the cells with anticancer drug, the ADR molecules which fail to be endocytosed in the cells will still be in the environmental solution and the electrochemical response of this part of the molecules can be readily detected. As shown in Figure 6A, the peak current of ADR was found to have a more considerable decrease in the presence of the c-SWNTs and AuNPs-gelatin nanocomposites than that without the nanocomposites.

(50) Jiang, H.; Wang, X. M. *Electrochem. Commun.* **2009**, *11*, 126–129.

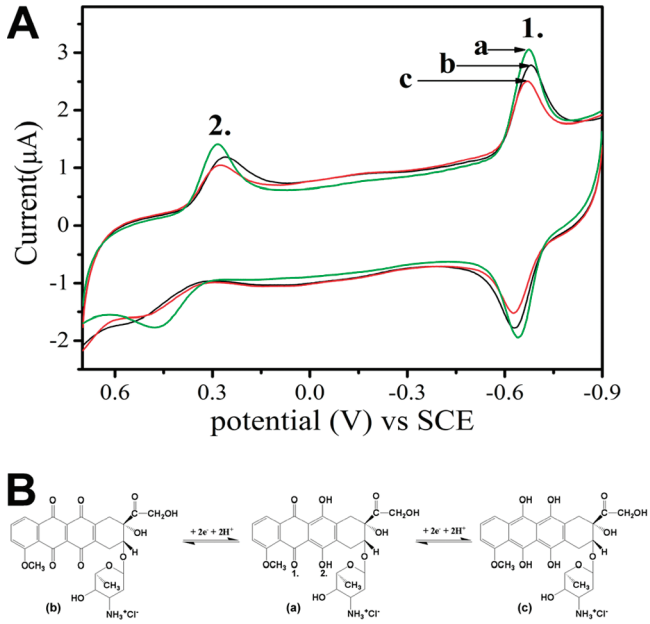

Figure 6. (A) Electrochemical detection of ADR (6.7 μg mL^{-1}) alone (a) and ADR residues outside the cells in the absence (b) and presence of c-SWNTs and AuNPs-gelatin (c). All concentrations of drugs and nanoparticles are the same as those in Figure 5. Scan rate: 100 mV s^{-1}. (B) Electrode reactions of ADR (a) and its oxidized (b) and reduced (c) forms. The numbers mark quinone and hydroquinone redox centers.

This suggests that much more ADR molecules have been accumulated into the cancer cells when combined with the nanocomposites. This phenomenon is consistent with our observations of inverted fluorescence microcopy and MTT assays, implying the possible cooperative effect of the nanocomposites to facilitate the uptake of anticancer drug ADR into the targeted tumor cells.

The possible mechanism of the enhanced effect on the drug uptake of ADR in target cancer cells by using the nanocomposites is shown in Scheme 2. As is known, the c-SWNTs are negatively charged due to the carboxyl groups on their surface. Hence, the positively charged ADR could be adsorbed on the surface of c-SWNTs by electrostatic interactions and assembled as a nanocomposite, leading to the enrichment of drug to a certain extent. On the other hand, as the nanoparticles could provide a versatile nanoscale surface for biomolecular recognition, the gelatin shell with the AuNPs may help them inlay into the bilayer phospholipids membrane. Meanwhile, the gelatin molecules is positively charged in neutral solution below the isoelectric point ($\sim$ 9.0), which results in the electrostatic interaction as well as other possible cooperation binding forces between the AuNPs-gelatin and negatively charged ADR-enriched c-SWNTs. Therefore, because of the presence of c-SWNTs and AuNPs-gelatin, the ADR molecules may have enhanced binding affinity to the cell membrane of the leukemia HL-60 cells, which could further lead to a

Scheme 2. Schematic Illustration of the Enhanced Effect on the Drug Uptake of ADR

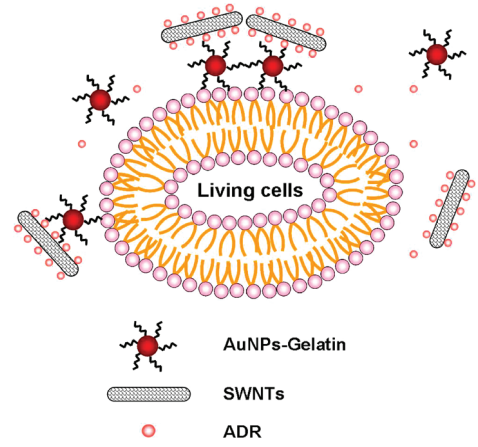

remarkably increased diffusion of anticancer agents across the plasma membrane of the cancer cells. This mechanism is similar to that of the daunorubicin-loaded nano Fe_3O_4 and polylactide nanofibers nanocomposites.[51]

CONCLUSIONS

This research describes the preparation of a novel nanocomposite of c-SWNTs-AuNPs-gelatin and the fabrication of a sensitive impedance sensor for the detection of cells. The nanocomposites showed excellent biocompatible spatial structure and nontoxic support for the adhesion and immobilization of HL-60 cells. More importantly, the MTT assay results indicated that the novel nanocomposites could facilitate the interaction of anticancer drug ADR to targeted cancer cells with enormous enhancement of the accumulation of anticancer drug in the individual leukemia cell. This makes the nanocomposites to be the ideal candidates for the enhancement of targeting efficiency in drug delivery. Thus, our results provide a new perspective for cancer chemotherapy.

ACKNOWLEDGMENT

We greatly appreciate the support of the National Natural Science Foundation of China for the Key Program (Grant 20635020) and the Creative Research Group (Grant 20821063). This work is also supported by National Basic Research Program of China (Grant 2006CB933201).

SUPPORTING INFORMATION AVAILABLE

Additional information as noted in text. This material is available free of charge via the Internet at http://pubs.acs.org.

Received for review March 26, 2009. Accepted June 30, 2009.

AC900628Y

(51) Gang, Lv.; He, F.; Wang, X. M.; Gao, F.; Zhang, G.; Gu, Z. Z.; et al. *Langmuir* **2008**, *24*, 2151–2156.